A new model for the resistance anomaly in mesoscopic superconducting wires

1994 J. Phys.: Condens. Matter 6 7055

(http://iopscience.iop.org/0953-8984/6/35/013)

J. Phys.: Condens. Matter 6 (1994) 7055–7062. Printed in the UK

A new model for the resistance anomaly in mesoscopic superconducting wires

Ju-Jin Kim†, Jinhee Kim†, Hyun Joon Shin†, Hu Jong Lee†, Seongjae Lee‡, Kyoung Wan Park‡ and El-Hang Lee‡

† Department of Physics, Pohang University of Science and Technology, Pohang 790-600, Korea

‡ Basic Research Department, Electronics and Telecommunications Research Institute, Daejeon 305-606, Korea

Received 13 September 1993, in final form 13 May 1994

Abstract. We propose a model that provides, for the first time, a quantitative explanation for the anomalous resistance peak in the superconducting transition of mesoscopic metal wires and loops. We assume a normal-current path in parallel with a normal–superconducting–normal quasi-particle tunnel barrier forming at the node area of the dangling voltage probes. The model allows a quantitative fit to the dependence of the resistance anomaly on the external parameters, such as temperature, bias current, and an external magnetic field.

Recently, anomalous resistance peaks above the normal-state value near the superconducting transition temperature have been observed in mesoscopic one-dimensional (1D) metal wires and loops [1–3], and in two-dimensional films [4, 5]. The observed characteristics of the anomaly in the mesoscopic systems can be summarized as follows [1–3]; (1) the anomalous resistance peak becomes smaller and broader as the samples become larger; (2) the magnitude of the anomaly decreases with increasing applied transverse magnetic field, vanishing completely in a relatively low field ($H \approx 20$ G); and (3) an external current tends to suppress the anomaly.

Close to the transition temperature, the superconducting coherence length $\xi(T)$ becomes very large, rendering the mesoscopic wires and loops essentially one dimensional. Fink and Grünfeld [6] showed that, in a current-carrying state, a 1D wire with a dangling side branch longer than $\xi(T)$ has an enhanced superconductivity (SC) over the range of $\xi(T)$ at the node (to be called 'node-superconductivity' (NSC) in the remainder of this paper). The NSC region forms as the SC in the middle of the wire is partly suppressed by the external current, whereas at the node the SC is relatively less suppressed over the range of superconducting coherence length $\xi(T)$ due to the proximity of the dangling branches carrying no current. The picture is valid as long as the level of the external current in the wire is much smaller than the middle-wire critical current $I_{c,wire}(T)$, which is in turn smaller than the critical current of the NSC region, $I_{c,node}(T)$.

However, for a current in the range $I_{c,wire}(T) < I < I_{c,node}(T)$ the SC survives only over a small region at the node areas. In this case, a normal–superconducting–normal (N–S–N) junction may form at the node, which may shrink with increasing current to a size even smaller than $\xi(T)$. It is known that a normal current injected from the metallic side of a normal–superconducting (N–S) interface is converted into a supercurrent within the charge imbalance relaxation length, λ_Q^* [7, 8]. Since the length can be as long as a few μm in a

0953-8984/94/357055+08$19.50

temperature range close to the transition of the NSC, the N–S interfaces tend to extend deep into the superconducting region.

It has been speculated that the interfacial resistance caused by this non-equilibrium effect at the junction may explain the resistance anomaly (RA) of the mesoscopic wire systems [1, 4, 8]. The resistance of a N–S interface is given by $R_Q = (2R_\square/W)(1 - \pi\Delta(T)/4k_BT)\lambda_Q^*(T, I, H)$, [7–9], where $R_\square$ and W are the sheet resistance and the width of the wire, respectively. $\Delta(T)$ is the gap in the NSC region, I is the total bias current, and H is a transverse external magnetic field. As pointed out in [1], however, the charge-imbalance effect at a N–S interface is not sufficient to explain the observed anomaly. Santhanam *et al* [1] also speculated that the RA they observed may have resulted from the charge-imbalance effect at the N–S interfaces of the voltage probes, once $\lambda_Q{}^*(T)$ became larger than the inter-probe distance. Although the assumption gave a qualitative explanation for the negative magnetoresistance observed in mesoscopic systems, no quantitative fit was given [10].

In order to solve the standing mystery of the RA we propose a simple model for the current flow pattern at the node of a voltage probe in a current-carrying mesoscopic wire. The model allows, for the first time, a quantitative explanation for the RA observed in mesoscopic wires and loops. For a given sample current I, we assume that the RA takes place in a temperature range $T_{c,wire}(T) < T < T_{c,node}(I)$, with the SC surviving only in the node areas. Note that, in any finite current, the node areas have a higher transition temperature $T_{c,node}(I)$ than that of the middle of the wire $T_{c,wire}(I)$. The temperature range specified above is equivalent to the current range $I_{c,wire}(T) < I < I_{c,node}(T)$ at a given temperature. Once the current exceeds $I_{c,wire}$, the range of the NSC cannot scale indefinitely with $\xi(T)$ as its transition temperature $T_{c,node}$ is approached from below, due to a simultaneous decrease of its critical current $I_{c,node}$. Thus we assume in the model that the NSC forms only over the range of the width of the voltage probe W (the same as the width of the wire itself for our sample). In this sense, our model predictions are in contrast to those of Fink and Grünfeld, which are valid when the bias current is smaller than $I_{c,wire}$. We also note that, contrary to the assumption in [1], no phase coherence exists between the voltage probes, due to the presence of the inter-probe normal region (see figure 1).

We consider a narrow temperature range $T_{c,wire}(T) < T < T_{c,node}(I)$ (for the details of the numerics of $T_{c,wire}(I)$ and $T_{c,node}(I)$ refer to table 1), where λ_Q^* is larger than the size of the NSC. Since $\Delta(T)/k_BT \ll 1$ in this range, most of the current tunnelling through the extended N–S–N junction remains as a quasi-particle current over the superconducting node, presumably with a small probability of Andreev reflection [11]. As a result, the superconducting gap in the node induces a mismatch in the quasi-particle conduction levels at the N–S interfaces and effectively reduces the N–S–N junction to a conduction tunnel barrier *with the junction resistance higher than the normal-state resistance*. Santhanam *et al* have also observed tunnel-junction-like behaviour with high effective tunnel barrier resistance in their wire samples [1].

For a current level above $I_{c,wire}(T)$ one may expect the SC in a node area itself to be partly destroyed, first in the side opposite to the dangling probe. This results, in each node, in the formation of a rectangular normal-current path of size $W \times W_n$ in parallel with an N–S–N quasi-particle tunnel barrier of length W, which protrudes the wire by $W–W_n$ (refer to figure 1). Since the barrier region exhibits a higher resistance than the normal region, the current flow in the temperature range $T_{c,wire}(I) < T < T_{c,node}(I)$ becomes highly non-uniform in the node region. The width of the normal-current path W_n is assumed to be self-adjusted so as to make the normal-current density $I_n(T)/W_n(T)$ identical to the critical-current density of the NSC, $I_{c,node}(T)/W$. Thus, the total current at a node is divided into

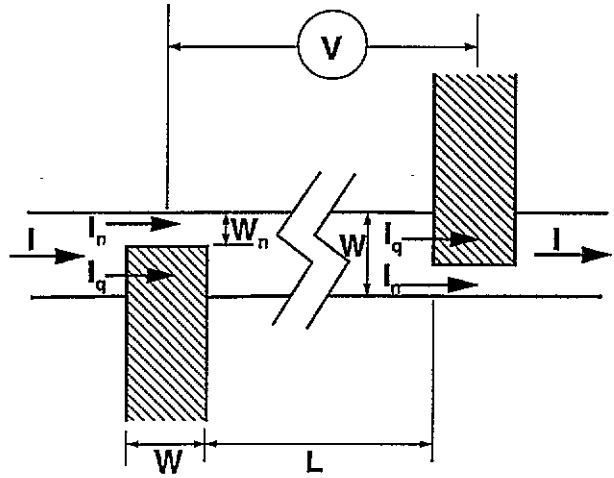

Figure 1. A schematic diagram of the current-flow pattern at the nodes of the voltage probes, which is used in deriving equation (1) and (2). The shaded area represents the region of enhanced superconductivity.

Table 1. Values of the parameters used in the fits to equation (2) of the bias-current dependence of the RA as shown in figure 3. The onset temperature of the RA, $T_{c,node}(T)$, is determined by the temperature best satisfying the relation $I_{c,node}(T) = I_{c,node}(0)[1 - \{T/T_{c,node}(0)\}^{3/2}] = I$, with $I_{c,node}(0) = 1126\ \mu A$.

I (μA)	R_n (Ω)	$T_{c,wire}(I)$ (K)	$T_{c,node}(0)$ (K)	$T_{c,node}(I)$ (K)	α	$\gamma\ (=\pi\xi(0)/L)$	β
0.5	8.67	1.341	1.397	1.389	0.164	1.54	1.500
1.0	8.67	1.329	1.398	1.385	0.160	1.54	1.498
2.5	8.67	1.298	1.398	1.374	0.126	1.54	1.497
5.0	8.76	1.271	1.397	1.359	0.055	1.51	1.498

the normal component through the normal-current path, $I_n = [W_n(T)/W]I_{c,node}(T)$, and the quasi-particle component through the barrier, $I_q(T)$. We assume the temperature dependence of $I_{c,node}$ to be in the 1D limit of the form $I_{c,node}(T) = I_{c,node}(0)[1 - T/T_{c,node}(0)]^{3/2}$ (see [12]), where $I_{c,node}(0)$ is a fitting parameter. The voltage drop across the barrier, which is identical to that across the normal-current path, is then given by the simple form

$$V_{node} = I_n(W/W_n)R_{\square} = I_{c,node}(T)R_{\square} \tag{1}$$

which is valid for $I < I_{c,node}(T)$. If $I_{c,node}(T)$ becomes smaller than the bias current I, upon approaching $T_{c,node}(0)$ from below, equation (1) should be replaced by $V_{node} = IR_{\square}$. Thus, we believe that the onset of the RA for a given I takes place at $T_{c,node}(I)$ [13]. A node, then, contributes an additional resistance $R_{node} = [I_{c,node}(T)/I]R_{\square}$ to the sample resistance, which gives rise to the RA. The resulting total resistance becomes $R_{total} = R_n + R_{node} = R_n[1+\alpha(W/L)\{I_{c,node}(T)/I\}]$ in the temperature range $T_{c,wire}(I) < T < T_{c,node}(I)$. Here, L is the inter-probe distance and the parameter α, which is supposed to be of order 1, reflects an uncertainty in estimating the geometrical factors. R_n ($\approx (L/W)R_{\square}$) is the normal-state resistance of a loop excluding the node regions [14]. If the fluctuation-superconductivity effect [15] in the normal-state area is taken into account the total resistance of a mesoscopic wire or a loop near the SC transition is given by

$$R(T)/R_n = \left[1 + \alpha W I_{c,node}(T)/LI\right]/\left[1 + G_{AL}R_n\right] \tag{2}$$

which explains well the anomalous resistance increase that occurs in the temperature range $T_{c,wire}(I) < T < T_{c,node}(I)$. Here, $G_{AL} = \gamma e^2/16h)[T/\{T - T_{c,wire}(I)\}]^{\beta}$ is the Aslamasov–Larkin fluctuation-enhanced conductance [15] with γ equal to $\pi\xi(0)/L$. Since the second term in the square bracket corresponds to the RA, one can see that it diminishes for longer samples and larger currents, as previously observed. For longer samples, the RA becomes smaller since the length of the constricted normal-current path at the nodes relative to the inter-probe distance becomes smaller, and the larger bias current widens the normal-current path, causing the RA to decrease.

In this study we prepared a mesoscopic square aluminium loop of the outer size about 0.9×0.9 μm^2, with the line width $W \approx 2000$ Å, and the inter-probe distance $L \approx 1.2$ μm. The loop was patterned on a SiO_2 (900 Å)/Si substrate with single-layer resist by electron beam lithography, followed by etching of the patterned SiO_2 layer for an overhang structure. An aluminium layer 200 Å thick was deposited by vacuum thermal evaporation of high-purity (99.999%) aluminium, followed by a lift-off process. The electrical contact was made by indium pressing on the electrodes. For measurements, we have adopted a four-terminal AC balance-bridge circuit consisting of a lock-in amplifier, operating at 33 Hz, and two differential preamplifiers. In order to protect the sample from accidental discharge we connected 1 kΩ metal-film resistors at each electrical lead. The sheet resistance of the film at 4.2 K is about 1.77 Ω/□. The resistance ratio R(300 K)/R(4.2 K) is 2.08. The zero-temperature coherence length estimated from the critical-field measurements is $\xi(0)$ = 907 Å. The charge-imbalance relaxation length is estimated to be $\lambda_Q^* \approx 5$ μm at a temperature given by $\Delta(T)/k_BT = 0.1$, which is approximately the lower bound of the temperature for the RA.

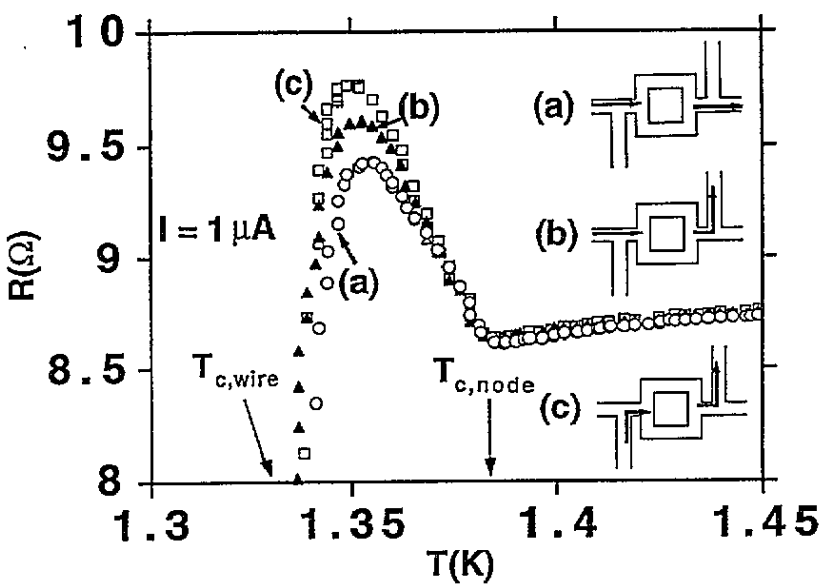

Figure 2. The dependence on the measurement configuration of the resistance anomaly. It clearly indicates that the anomaly is closely related to the current-flow pattern near the nodes of the voltage probes.

Figure 2 shows the dependence on the current path of the RA obtained with a bias current $I = 1$ μA. The maximum value of the RA above the normal-state resistance R_n in the range $T_{c,wire}(I) < T < T_{c,node}(I)$ corresponds to 9–13% of R_n. Note that, for the

different measurement configurations, only the magnitude of the peak changes, without noticeable changes in either the normal-state resistance or the two critical temperatures, $T_{c,wire}$ ($\approx$ 1.330 K) and $T_{c,node}$ ($\approx$ 1.380 K). The behaviour shown in figure 2 strongly indicates that the RA is closely related to the current-flow pattern in the sample. A change in the measurement configuration alters the boundary conditions for the current flow at the nodes. We suppose that the normal current flows through the outer region (opposite side of the dangling probe) of the wire at the nodes for configuration (a), whereas it may flow along the inner side of the corners at one of the nodes for configuration (b) and at both nodes for configuration (c). Although it is not obvious, the normal-current channel becomes more constricted and/or longer for configurations (b) and (c), resulting in higher RA than for configuration (a).

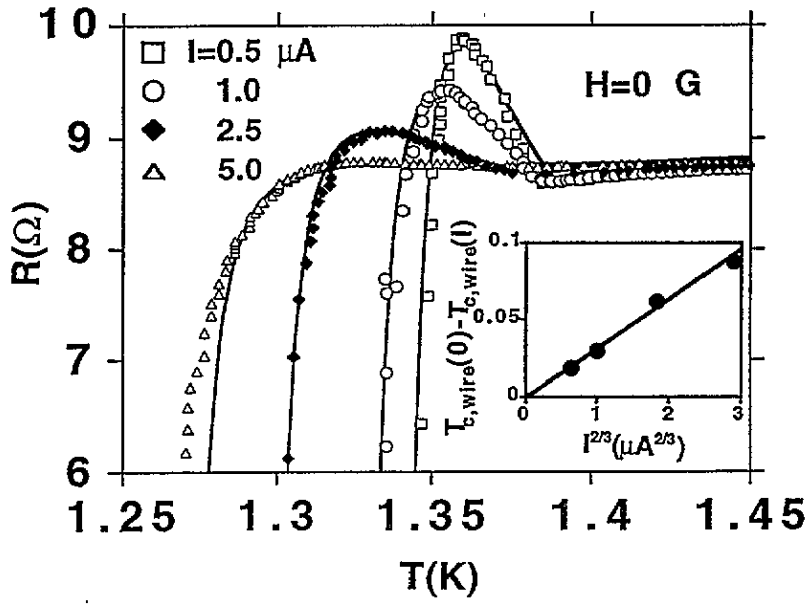

Figure 3. The dependence on the bias current of the resistance anomaly. The solid curves represent best fits to equation (2) using the parameters shown in table 1. The inset shows the decrease of $T_{c,wire}$ with a bias current, which follows well the 1D relation, $T_{c,wire}(0)-T_{c,wire}(I) \sim I^{2/3}$. The solid line represents the best-fit line.

Figure 3 shows the bias-current dependence of the RA. The abrupt increase of the resistance at $T_{c,node}(I)$ in the presence of a small bias current is due to a constriction of the normal-current path by the formation of the N–S–N quasi-particle tunnel barriers at the nodes with effective sheet resistance larger than $R_{\square}$. Further increases in the bias current cause the width of the normal-current path to expand, and suppress the magnitude of the anomaly. Notice that the onset temperature of the anomaly $T_{c,node}(I)$, shown in the figure, decreases only slightly as the current level increases by a factor of 10, while the superconducting phase boundary $T_{c,wire}(I)$ decreases considerably. The solid curves in figure 3 represent a numerical fit to equation (2) with the parameter values listed in table 1. In the fit, we used $I_{c,node}(0)$ = 1.126 mA (corresponding to 2.8×10^7 A cm^{-2}) for all bias currents, which were determined for best fit, especially for best fit of the onset temperature of the RA, $T_{c,node}(I)$. The best-fit value of R_n ($\approx$ 8.7 Ω) is very close to the measured one (8.85 Ω) with the spread in $T_{c,node}(0)$ (= 1.397–1.398 K) for the different bias currents within 1 mK, verifying the self-consistency of the fit. The suppression of the superconducting phase boundary of

the loop $T_{c,wire}(I)$ in a bias current follows the well known relation valid for 1D wire [16], $\Delta T_{c,wire} = T_{c,wire}(0) - T_{c,wire}(I) \sim I^{2/3}$, as shown in the inset to figure 3. It is clear from the value of $\beta \approx 3/2$, that the Aslamasov–Larkin fluctuation-enhanced conductivity fits the 1D expression [15] well, as assumed in the study. The best-fit value of $\gamma = 1.51$–1.54 turns out to be about 6.4 times larger than that estimated from the relation $\gamma = \pi\xi(0)/L = 0.237$. This result is consistent with the much larger fluctuation conductivity compared to the Aslamasov–Larkin prediction, as observed previously in clean aluminium films [17]. The data for $I = 5$ μA tend to deviate from the fit near $T_{c,wire}(I)$, which may be caused by a high-bias current-flow pattern which cannot be described by the rigid-boundary model with the simple geometry.

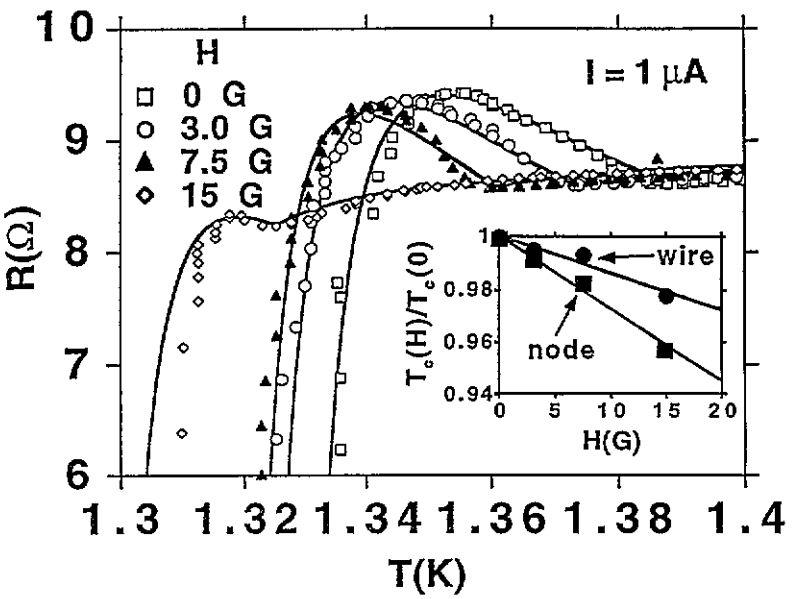

Figure 4. The dependence on the magnetic field of the anomaly for a bias current of $I = 1$ μA. The solid curves show best fits to equation (2) using the parameters listed in table 1 (except for α; see the text), and with a field dependence of the $T_{c,node}$ and $T_{c,wire}$. The inset shows linear field suppression of $T_{c,node}(H)/T_{c,node}(0)$ (squares) and $T_{c,wire}(H)/T_{c,wire}(0)$ (circles).

The magnetic field dependence of the RA for a fixed bias current can also be well explained in terms of our model, as shown in figure 4 (with $I = 1$ μA). In contrast to the case of the current dependence, however, both $T_{c,wire}(I, H)$ and $T_{c,node}(I, H)$ decrease considerably with increasing magnetic field. The decrease of the onset temperature of the RA implies a decrease of $T_{c,node}(I, H)$ in a field. This is consistent with a field suppression both of the node superconductivity and of the fluctuation superconductivity in the loop itself. As the magnetic field is increased, the anomaly is gradually suppressed and disappears almost completely for $H = 15$ G. The solid curves in figure 4 represent a fit of the field dependence of the RA to equation (2) in $I = 1$ μA, when the field suppression of $T_{c,wire}(I, H)$ and $T_{c,node}(I, H)$ is taken into account. In the fit, we used the same values for the zero-field parameters as listed in table 1, except for the geometry parameter α which changes to 0.20, 0.28 and 0.30 for fields of 3 G, 7.5 G and 15 G, respectively. The inset shows that the best-fit values of the critical temperatures $T_{c,wire}(I, H)$ and $T_{c,node}(I, H)$ decrease linearly with field, which suggests a field dependence of the critical temperatures of the form [18], $T_{c,wire}(H) \approx T_{c,wire}(0)[1 - H/H_{c,wire}(0)]$ and $T_{c,node}(H) \approx T_{c,node}(0)[1 - H/H_{c,node}(0)]$. The

slopes of the best-fit lines shown in the inset, together with the field dependence above, give $H_{c,wire}(0)$ = 705 G and $H_{c,node}(0)$ = 361 G. The fit shows excellent quantitative agreement with the data. Note that, with increasing magnetic field, the field dependence of the critical temperatures results in a smaller difference between the two critical temperatures, so they merge almost completely for a field larger than ~20 G. The behaviour agrees well with the experimental results.

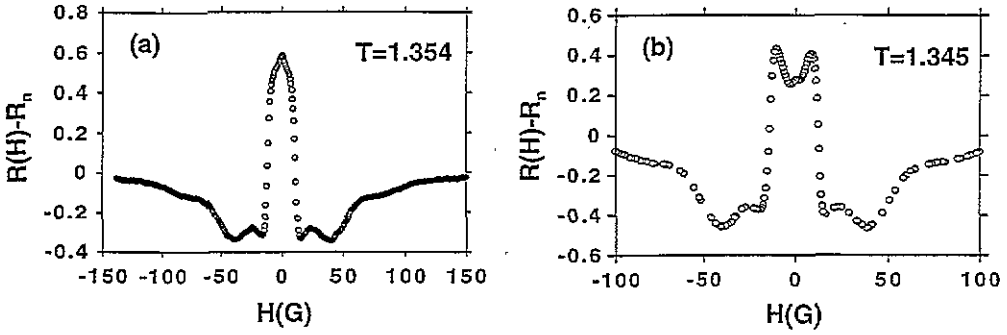

Figure 5. The magnetoresistance taken with I = 1 μA; (a) at T = 1.354 K, the temperature of the peak of the zero-field RA, (b) at T = 1.345 K, the temperature slightly above $T_{c,wire}$.

We have also measured the magnetoresistance (MR) of the loop with I = 1 μA at various temperatures near $T_{c,wire}$ (= 1.329 K). As shown in figure 5 (a), at the temperature corresponding to the peak of the zero-field RA (T = 1.354 K), we observed a sharp peak in the MR in the low-field region, $|H|$ <15 G, superimposed on a small positive MR. As the temperature decreases toward $T_{c,wire}$, however, the MR peak starts to collapse near H = 0, resulting in a large zero-field dip in the MR at temperatures very close to $T_{c,wire}$ (figure 5(b)). One can explain the behaviour [19] in terms of the combined effect of field dependences of the NSC and the phase-coherence effect due to fluctuation superconductivity in the loop in the temperature range $T_{c,wire} < T < T_{c,node}$. The suppression of the NSC gives a negative MR due to an expansion of the normal-current path with an external field as the critical current of NSC decreases. The effect dominates the low-field ($|H|$ <15 G) MR at the temperatures near the zero-field anomaly peak. By contrast, the field suppression of the fluctuation superconductivity gives the positive MR background with small oscillations caused by the phase-coherence effect, which is seen in figure 5 for $|H|$ >15 G where the NSC effect becomes relatively small. The magnitude of the external field corresponding to one flux quantum threading the loop, 42 G, is close to the observed period of the background oscillations, 41 G, as in figure 5. When approaching $T_{c,wire}$, the change in this positive MR for $H \approx 0$ becomes very steep, causing a zero-field dip as shown in figure 5(b). Preliminary results of our analysis indicates that the anomalous Little–Parks oscillations [2] observed very recently in mesoscopic aluminium loops below $T_{c,wire}$ may also be interpreted in terms of our model, provided the superconducting phase-coherence effect is incorporated into the model. The details of the explanation for the MR behaviour will be presented separately.

In conclusion, the essential feature of our RA model is the assumption that a normal-current path forms at the node of the voltage probes in parallel with the existing quasi-particle tunnelling path arising from the enhanced superconductivity at the node. The anomalous increase of the resistance is caused by a constriction of the normal-current path with an increased current density due to the presence of the higher-than-normal tunnelling resistance in the N–S–N barrier. The dependence on external parameters of the anomaly is,

then, a consequence of a change in the width of the normal-current path together with the magnitude of the normal current through it.

Acknowledgments

One of us (H J Lee) thanks Dr Soon-Gul Lee for various illuminating discussions on charge imbalance relaxation and Dr S E Hebboul for critical reading of the manuscript. We also thank S G Choi for technical assistance in sample preparation. This work was supported in part by Basic Science Research Centre administrated by the Ministry of Education, Korea, under Contract No N91126 and in part by Korea Science and Engineering Foundation, under Contract No K92099.

References

[1] Santhanam P, Chi C C, Wind S J, Brady M J and Bucchignano J J 1991 *Phys. Rev. Lett.* **66** 2254

[2] Vloeberghs H, Moshchalkov V V, Van Haesendonck C, Jonckheere R and Bruynseraede Y 1992 *Phys. Rev. Lett.* **69** 1268

[3] Kim J-J, Kim J, Lee S, Lee H J, Park K W, Shin H J and Lee E-H 1994 *Physica* B **194–196** 1035

[4] Kwong Y K, Lin K, Hakonen P J, Isaacson M S and Parpia J M 1991 *Phys. Rev.* B **44** 462

[5] Vaglio R, Attanasio C, Maritato L and Ruosi A 1993 *Phys. Rev.* B **47** 15 302

[6] *Fink H J and Grünfeld V 1985 Phys. Rev.* B **31** 600

[7] Skocpol W J 1981 *Nonequilibrium Superconductivity, Phonons, and Kapitza Boundaries* (New York: Plenum) p 559

[8] Santhanam P, Umbach C P and Chi C C 1989 *Phys. Rev.* B **40** 11 392

[9] The expression for R_Q holds for $\Delta/k_BT \ll 1$, which is satisfied at temperatures near the transition temperature of the NSC, $T_{c,node}$, as in our case. The assumption for the value of the ratio is also consistent with the negative magnetoresistance as observed in the current study.

[10] After completion of this study an alternative interpretation:
Hui V C and Lambert C J 1993 *J. Phys.: Condens. Matter* **5** L651; 1994 *Physica* B **194–196** 1637
has been proposed for a similar resistance anomaly observed in normal-metallic mesoscopic systems, proximity coupled to a superconductor; see
Petrashov V T *et al 1993 JETP Lett.* **58** 49
Here, the anomaly, either positive or negative in sign, was interpreted as a consequence of the competition between Andreev and normal scattering at N-S interfaces.

[11] Blonder G E, Tinkham M and Klapwijk T M 1982 *Phys. Rev.* B **25** 4515

[12] Since no expression for the temperature dependence of the critical current available for this non-equilibrium situation we adopted the 1D form. But there is no real relevance of using it. It turns out that, except for an appreciable change in $I_{c,node}(0)$, both the quality of the fit and the values of the other parameters are very insensitive to the choice of the different temperature dependence of $I_{c,node}$.

[13] In our model, the width of the normal current path W_n at a node can be expressed as $W_n = (R_q^{\square} I - R_{\square} I_{c,node})W/[(R_q^{\square} - R_{\square})I_{c,node}]$, where $R_q^{\square}$ (which is always larger than $R_{\square}$) is the effective sheet resistance of the extended quasi-particle tunnel barrier. As temperature increases W_n widens with a simultaneous increase in I_n ($= W_n I_{c,node}/W$). W_n and I_n become W and I, respectively, as the onset temperature of the RA is approached from below.

[14] For our loop sample R_n is expected to be only a little smaller (by about 15%) than that of a wire with the *same inter-probe distance and width as the loop.*

[15] See, for example,
Tinkham M 1975 *Introduction to Superconductivity* (New York: McGraw-Hill) p 254

[16] Pannetier B 1991 *Quantum Coherence in Mesoscopic Systems* (New York: Plenum) p 457

[17] Crow J E, Thompson R S, Klenin M A and Bhatnagar A K 1970 *Phys. Rev. Lett.* **24** 371

[18] The contradiction to the 1D quadratic field dependence of the critical temperature is not clear.

[19] Kim J-J, Kim J, Lee S, Lee H J, Park K W, Shin H J and Lee E-H 1994 *Physica* B **194–196** 1647